Multiple myeloma primary cells show a highly rearranged unbalanced genome with amplifications and homozygous deletions irrespective of the presence of immunoglobulin-related chromosome translocations

Cristina Largo, Borja Saéz, Sara Alvarez, Javier Suela, Bibiana Ferreira, David Blesa, Felipe Prosper, M. Jose Calasanz, Juan C. Cigudosa

From the Molecular Cytogenetics Group, Centro Nacional de Investigaciones Oncológicas (CNIO), Madrid, Spain (CL, SA, JS, BF, DB, JCC); Department of Genetics, University of Navarra, Pamplona, Navarra, Spain (BS, MJC); Area of Cancer, Area of Cell Therapy and Haematology Service, University Clinic, University of Navarra and Foundation for Applied Medical Research, Pamplona, Navarra, Spain (FP).

Acknowledgments: we thank Drs Marta R. Salazar (University Clínic, Pamplona), Maite Ardanaz (Hospital Txagorritxu, Vitoria), Jose Ferreiro (Hospital Donostia, San Sebastian), Filomena Floristán (Hospital de Cruces, Bilbao), Jose A Marquez (Hospital de Basurto, Bilbao), Carmen Mateos (Hospital Virgen del Camino, Pamplona), Ana Gorosquieta (Hospital de Navarra, Pamplona) and Gotzon Pereda (Hospital de Santiago, Vitoria) for kindly providing samples and clinical data. We are also grateful to M Carmen Martín Guijarro, Carmen Carralero and Gloria Soler for their excellent technical support.

Funding: CL and BS have PhD fellowships from Gobierno de Navarra. JS has a PhD fellowship from Ministerio de Educación y Ciencia. BF has a Marie Curie PhD Early Stage Research Training Fellowship. Work funded by Red Temática FIS G03/136 Mieloma Múltiple y otras Ganmapatías: de la Génesis a la Terapéutica and by Grant PI040555 from Fondo Investigaciones Sanitarias, Ministerio de Sanidad y Consumo to JCC.

Manuscript received November 16, 2006.
Manuscript accepted March 15, 2007.

Correspondence:
Juan C. Cigudosa, PhD, Molecular Cytogenetics Group, Centro Nacional de Investigaciones Oncológicas (CNIO), Melchor Fernández Almagro 3, 28029 Madrid, Spain.
E-mail address: jccigudosa@cnio.es

ABSTRACT

Background and Objectives

Multiple myeloma (MM) is a malignant plasma cell neoplasia in which genetic studies have shown that genomic changes may affect almost all chromosomes, as shown by fluorescence *in situ* hybridization (FISH) and comparative genomic hybridization (CGH). Our objective was the genomic characterization of CD 138 positive primary MM samples by means of a high resolution array CGH platform.

Design and Methods

For the first time, a high resolution array CGH with more than 40,000 probes, has been used to analyze 26 primary MM samples after the enrichment of CD138-positive plasma cells.

Results

This approach identified copy number imbalances in all cases. Bioinformatics strategies were optimized to perform data analysis allowing the segregation of hyperdiploid and non-hyperdiploid cases by array CGH. Additional analysis showed that structural chromosome rearrangements were more frequently seen in hyperdiploid cases. We also identified the same Xq21 duplication in nearly 20% of the cases, which originated through unbalanced chromosome translocations. High level amplifications and homozygous deletions were recurrently observed in our series and involved genes with meaningful function in cancer biology.

Interpretation and Conclusions

High resolution array CGH allowed us to identify copy number changes in 100% of the primary MM samples. We segregated different MM subgroups based on their genomic profiles which made it possible to identify homozygous deletions and amplifications of great genetic relevance in MM.

Key words: multiple myeloma, arrayCGH, hyperdiploid, amplification, homozygous deletion.

Haematologica 2007; 92:795-802

Multiple myeloma (MM) is an incurable malignant plasma cell (PC) neoplasia characterized by the accumulation of malignant plasma cells in the bone marrow. There is a wide variability in clinical features, responses to treatment, and survival times among patients.[1] Chromosome aberrations, present in virtually all patients with MM[2] include chromosome translocations involving the *IG* loci and/or copy number changes of partial or whole chromosomes.[3] Two major genetic subtypes of MM have been defined: the hyperdiploid variant (H-MM), associated with multiple chromosome trisomies, and the non-hyperdiploid variant (NH-MM) with a high prevalence of *IGH* translocations.[4] This classification seems to have relevance in prognosis since, recently, H-MM has been associated with a better survival and a similar response rate to treatment when compared to NH-MM.[5]

Chromosome-based comparative genomic hybridization (CGH) has shown that DNA copy number variations (CNV) in MM may affect almost all chromosomes.[6-8] We recently found, by array-based CGH (array CGH) CNV that resulted in the overexpression of genes included in amplified chromosomal regions.[9] Here, we characterized CNV in a panel of CD138-enriched primary MM samples with high density array CGH.

Design and Methods

Patients and molecular cytogenetics

DNA from $CD138^+$ cells, isolated from the bone marrow of 26 cases of MM at diagnosis, by means of magnetic cell sorting (Miltenyi Biotec, Aubum, CA, USA), was studied. DNA was extracted using DNeasy tissue kits (Qiagen, Germantown, MD, USA). All samples were enriched to more than 70% plasma cells (median 95%) (*Supplementary Table 1*). The median age of the patients from whom the sampes were obtained was 67.5 years (range: 34-85). There were 16 men and 10 women in our series. Most patients (22/26) were homogenously treated with the GEMM2000 protocol designed by the Spanish GEM-PETHEMA group (Table 1). All samples were collected after proper informed consent. All samples were cytogenetically characterized: 85% showed a normal karyotype. We screened our series by fluorescence *in situ* hybridization (FISH) with *IGH* (Vysis, Downers Grove, IL, USA) and IGL^{10} break-apart probes. Nine samples (34.6%) showed *IGH* rearrangements and two (7.7%) had *IGL* rearrangements.

Reference genomic DNA

Genomic DNA was obtained from peripheral blood of ten healthy female donors. DNA was extracted using a standard saline precipitation method and was purified by phenol-chloroform extraction using Light Phase-Lock Gel tubes (Eppendorf AG, Hamburg, Germany). The same amounts of each donor DNA were mixed in a female DNA pool for use as reference DNA in all hybridizations.

Array CGH assays

Human Genome CGH 44k microarrays (Agilent Technologies, Palo Alto, CA, USA) were used in this study. This platform consists of approximately 44000 60-mer oligonucleotide probes that span the human genome with an average resolution below 50 Kb. The platform has gene focused coverage in order to ensure adequate coverage in most commonly studied genomic regions. Array CGH assays were performed as previously described[11] with minor modifications. The DNA pool from ten helathy females was used as the reference DNA for all hybridizations. Slides were scanned using an Agilent 2565AA DNA Microarray Scanner (Agilent Technologies). Raw data can be freely accessed via our ftp server at *www.cnio.es*.

Images and data analysis

Microarray images were transformed to fluorescence intensities using Feature Extraction Software, version 8.1 (Agilent Technologies). Data were analyzed using Agilent CGH Analytics 3.2.25 software. Quality criteria were a derivative log ratio (DLR) spread lower than 0.3 log units and a signal to noise ratio for each channel greater than 30. DLR spread metrics estimates the log ratio noise by calculating the spread of log ratio differences between consecutive probes along all chromosomes. In order to establish gained and lost regions, a 500 Kb weighted moving-average window and a ζ-score threshold of±2.5 were used. ζ-score values were obtained for each probe and were categorized into gains and losses. Using this threshold, high level amplifications were defined as consecutive clones, spanning a region, which showed a $\log_{10}$ ratio higher than 0.3 (more than five copies) within a gained region and homozygous deletions as consecutive clones with a $\log_{10}$ ratio lower than -1 (no copies) and detected as losses by ζ –score. Those aberrant regions that did not reach these cut off values were considered low copy gains or single losses. For the subsequent analyses, regions of gains and losses were established. A region is defined as a group of at least three consecutive probes that are simultaneously and similarly changed.

Aberrations were categorized as numerical and structural changes. The latter type was divided into changes greater than 3Mb (>3Mb) and those less than 3Mb (<3Mb) regarding high resolution conventional CGH resolution (*detailed data are provided in Supplementary Table 3*).

Identification of H-MM and NH-MM

H-MM and NH-MM were easily classified in our series by array CGH. Based on the array CGH profile a copy number score (CNS) value was assigned to each chromosome. When there was not a whole chromosome gain or loss, a CNS value of 2 was assigned, when an entire chromosome gain occurred, a CNS of 3 was assigned and, finally, when a loss occurred the CNS was equal to 1. The sum of CNS values of each case was calculated and if the value was from 48 to 74 the case was classified as H-MM; when a different CNS was obtained, it was considered

Table 1. General features of the multiple myeloma samples included in the study.

Case	M/F (age)	Treatment	Response	Karyotype	FISH Ig t	Ploidy	Array CGH 13q-	1q+	dup Xq
1	M(78)	GEMM2000	No	46,XY/45,X,-Y	–	H	–	–	–
2	M(66)	GEMM2000	No	46,XY	–	H	–	–	+
3	M(39)	GEMM2000	Yes	46,XY	IGH+	NH	–	–	–
4	M(61)	GEMM2000	Yes	46,XY	–	NH	–	+	+
5	F(67)	NT	x	46,XX	–	NH	–	–	–
6	M (71)	GEMM2000	No	46,XY	IGH+	NH	+	+	–
7	M (73)	GEMM2000	No	46,XY	IGH+	NH	–	–	–
8	F (75)	NT	x	46,XX	–	NH	+	–	–
9	M(68)	GEMM2000	NO	57,XY<3n>, -1,der(6)t(1q;6q)x2,-8,-13,-14,-16,-17,-18,-20	IGL+	H	–	+	–
10	M(70)	GEMM2000	Yes	46,XY	–	H	+	–	–
11	M(72)	GEMM2000	Yes	46,XY	IGL+	H	+	+	+
12	M(58)	GEMM2000	Yes	46,XY	–	NH	+	+	–
13	F(34)	GEMM2000	Yes	NA	IGH+	NH	+	–	–
14	F(67)	GEMM2000	Yes	46,XX	IGH+	NH	–	–	–
15	M(57)	GEMM2000	Yes	46,XY	IGH+	NH	+	–	–
16	M(67)	Thalidomide vs placebo	Yes	46,XY	–	NH	–	–	–
17	F (52)	GEMM2000	Yes	46,XX, inv(9)(q11q13) [100%]	–	H	–	+	–
18	M(85)	NT	x	46,XY	–	H	–	–	–
19	F (62)	GEMM2000	Yes	46,XX	–	H	+	+	+
20	M (59)	GEMM2000	No	46,XY,der(1p),+3,+5, der(8p),der(9p),- 13,add(13p), add(14)(q32), +15,er(16q), der(20q),+mar [100%]	–	H	+	+	+
21	F (66)	GEMM2000	Yes	46,XX [67%]50,XX, add(1)(p36), der(3q), t(3;3)(q?;q?), +7,add(12)(p13), der(14q),+mar [33%]	–	H	–	–	–
22	F(71)	GEMM2000	Yes	46,XX	IGH+	NH	+	–	–
23	M(73)	GEMM2000	Yes	46,XY	–	H	–	–	–
24	M(81)	GEMM2000	Yes	46,XY	IGH+	H	–	–	–
25	F(74)	GEMM2000	Yes	NA	IGH+	NH	–	+	–
26	F(54)	GEMM2000	No	45,X,-X[87%] 51,XX,der(1)(p?), +3,+5,+7,+8,-9,+11,der(14)(q?), add(16)(p?),+18 [13%]	–	H	–	+	–

Besides clinical features, Ig translocation status (Ig t determined by FISH) and known genetic features (determined by array CGH) are shown. M: male; F: female; NT: not treated.

Table 2. Description of 68 recurrent SORI identified in the MM samples.

		Gains				Losses		
Chr	*Region*	*Start*	*Size (Mb)*	*%*	*Chr*	*Region*	*Start*	*Size (Mb)*	*%*
1	1q	142902432	102.520	38	1	1p36.32	1536308	5.000	8
3	3pter[1]	224727	3.337	35	1	1p36.12	23265113	0.604	8
3	3q11-q22[1]	108062308	32.496	38	1	1p33[3]	50669458	3.014	8
3	3q26-qter[1]	197698952	1.593	42	1	1p31.1[3]	80821425	2.856	12
5	5p-q13.2[1]	148243	73.955	38	1	1p21.3-p31.1	84171854	12.042	12
5	5q21.11q-ter[1]	96057266	84.560	38	1	1p12-p21.1	103799708	14.591	15
6	6p22.1-25.2	352463	26.129	23	3	3p24.3	24930353	0.880	12
6	6q12	64228424	3.086	15	4	4p16.2[3]	1661893	0.184	12
6	6q12	69403244	1.154	15	4	4p15.33[3]	13019621	0.285	12
7	7p21.1[1,2]	5637996	0.178	35	4	4p15.31-p15.1[3]	16751089	14.070	8
7	7p21.1[1,2]	11853187	0.515	35	4	4p13[3]	44691513	1.538	8
7	7p21.1[1,2]	16776548	0.337	31	4	4q13.2-q22.1	66059589	26.058	8
7	7p14.1[1,2]	36074495	0.333	35	6	6q23.2	136920041	0.341	12
7	7q[1,2]	61960303	96.628	27	6	6q26[3]	160608251	0.522	15
8	8q23.3-q24.21	117725989	8.097	12	7	7p22	1263119	0.093	8
8	8q24.21[3]	128548643	0.407	15	8	8p12-p22	13991907	13.105	27
9	9q22.2	89830592	1.734	42	8	8p11.22	37847079	0.527	19
9	9q34.2[1]	132972692	0.043	50	8	8q23.1	107376988	0.545	8
11	11q13.2-q13.4	68821295	7.553	31	9	9p21.3	21067574	0.786	8
11	11q23.2-qte[1]	114350685	19.601	35	11	11q22.1	100828925	1.492	8
15	15[1]	19109124	81.060	42	12	12p13.32	3509030	0.820	8
16	16q22.2	69322931	0.553	8	12	12p12.1	21152676	0.400	12
17	17p13.2	3632698	1.334	12	12	12q21.33	86882565	0.906	8
17	17p11	16763408	0.663	15	13	13q12.12	19140499	0.376	35
17	17q21.32	41458670	0.242	23	13	13q12-q21	45637710	20.455	38
18	18	170229	75.913	15	14	14q13.2-q21.3	30209271	16.915	12
19	19p13.12-pter[1]	232080	17.754	65	14	14q24.2	68763265	14.399	15
19	19q13	34522544	1.330	50	14	14q32.32	101569155	1.268	15
19	19q13.2[1]	42921103	0.673	50	16	16p13.2	3646249	0.601	8
20	20q11.22	31714033	0.387	8	16	16p13.12	13923497	0.026	23
21	21q21.1	15295891	4.694	12	16	16q24.2[3]	83644296	1.600	23
X	Xq21.333-q25	97661774	26.092	19	17	17p13.2-p12	7054388	9.209	15
X	Xq25-qter	126030916	28.374	19	20	20q12	37664253	0.577	8
					22	22q11.22	21004565	0.344	19
					22	22q12.1	22555378	5.501	23

[1]*SORI that were significantly (adjusted p-value <0.05) more frequent in the H-MM group than in the NH-MM group.* [2]*Statistically significant SORI identified in one of the H-MM groups.* [3]*SORI present in one of the NH-MM groups, but not statistically significant.*

NH-MM. Ploidy status was further confirmed by a standard FISH assay based on centromeric probes (Vysis, Downers Grove, IL, USA).

Definition of smallest overlapping regions of imbalance (SORI)

Genomic aberration region data were used to obtain the SORI. Each SORI represented the most recurrent region of imbalance whose limits were defined by the minimum number of clones with the highest percentage of recurrence.[12] SORI were defined independently for gains and losses. They were evaluated to define regions targeted by overlapping events in two or more samples. SORI limits were defined by the clones at the boundaries of the gained or lost region of the case showing the smallest unbalanced region. After SORI delimitation the presence or absence of belonging aberration was assigned to each sample (0=absence, 1=presence).

Bioinformatics and statistical analysis

GEPAS Suite software (*http://gepas.bioinfo.cipf.es/*) was used for unsupervised clustering, supervised analysis and gene annotation. A region was considered as statistically significant if the adjusted *p* value was below 0.05. For statistical comparison of the difference in the number of copy number changes in different groups, the U Mann-Whitney test was used with the SPSS v 13.0 package.

FISH and spectral karyotyping (SKY) analysis

FISH assays were carried out as described elsewhere.[13] In order to identify whether there were any translocations involving the immunoglobulin (Ig) heavy and light chain loci, FISH assays were conducted with LSI IGH Dual Color Break Apart probe and IGL break apart probe.[10] A non-commercial probe was used for the analysis of Xq21-qter duplication (*Supplementary Table 3*). Total Chromosome DNA X Probe (Qbiogene, Carlsbad, CA, USA) was used in combination with LSI IGH Dual Color Break Apart probe (Vysis), in order to study the involvement of *IGH* in Xq21 translocation. The probes used for the validation of amplification and homozygous deletions are described in supplementary Table 3.

SKY was carried out as previously described.[13,14] At least five metaphases were analyzed for each case.

Table 3. Description of amplifications and homozygous deletions identified in MM.

				Amplifications		
Chr	*Region*	*Start*	*Size (Mb)*	*Cases with HLA*	*% cases G*	*Genes in the region*
6	6q12	64228424	3.086	26	11.5	*PTP4A1, PHF3, LOC389405, EGFL11*
6	6q12	69403244	1.154	26	11.5	*BAI3, C6orf209*
9	9q22.2	89830592	1.734	4	30.8	*LOC340515, DIRAS2, SYK, BF510209, AUH, NFIL3, ROR2*
9	9q34.2	132972692	0.043	20, 191	42.3	*CEL, RALGDS*
14	14q21.1	44463153	0.372	14	0	*BTBD5,KIAA0423, PRPF39, FKBP3, C14orf106*
16	16q22.2	69441287	0.312	4	3.8	*HYDIN*
17	17p13.2	3632698	1.334	26	7.7	*HSA277841, CAMKK1, P2RX1, ATP2A3, ZZEF1, ANKFY1, UBE2G1, MYBBP1A, FLJ90165, ALOX15, PELP1, ARRB2, CXCL16, ZMYND15, TM4SF5, LOC284013, PSMB6, PLD2, MINK1, CHRNE, GP1BA, SLC25A11, RNF167, PFN1, ENO3, SPAG7, CAMTA2, INCA1, KIF1C, GPR172B, FLJ30726, ZNF232*
17	17p11	15589242	1.837	23, 261	7.7	*FLJ40244, ADORA2B, TTC19, NCOR1, PIGL, PRR6, TRPV2, FLJ35696, ZNF287, ZNF624, FLJ36492, TNFRSF13B, M-RIP, LOC201164, FLCN, COPS3, NT5M, MED9, RASD1, PEMT*
19	19q13	34522544	1.299	4	46.2	*LOC284395, POP4, PLEKHF1, C19orf12, CCNE1, C19orf2, ZNF536*

				Homozygous deletions		
Chr	*Region*	*Start*	*Size (Mb)*	*Cases with HD*	*% Hem.D.*	*Genes in the region*
6	6q26.2	137061308	0.199	4	7.7	*MAP3K5, PEX7*
11	11q22.1	100828925	1.491	2	3.8	*TRPC6, ANGPTL5, KIAA1377, YAP1, BIRC3, BIRC2, PORIMIN, MMP7, MMP20, MMP27, MMP8, MMP10, MMP1, MMP3, MMP12, MMP13*
13	13q12	19140499	0.376	20, 152	26.9	*HSMPP8, PSPC1, ZNF237, ZNF198*
22	22q11.22	20994020	0.354	12	15.4	*IGLC2, SUHW2, SUHW1, PRAME*
X	Xq21.31-21.33	86728457	10.933	4	0	*PABPC5, NAP1L3, FLJ37659, DIAPH2, CPXCR1, KLHL4, PCDH11X*
X	Xq25	123753696	2.090	4	0	*WDR40B*

[1]When recurrent amplification was revealed, the smallest overlapping region of amplification is described. [2]Case 23634 shows two consecutive clones homozygously deleted covering the ZNF198 gene locus. HLA: high level amplification; G: gain; HD: homozygous deletion; Hem. D: hemizygous deletion.

Results

A high number of genomic aberrations were found in MM

The presence of DNA copy number changes in 26 primary MM samples was analyzed by high resolution array CGH. Most of the samples had a normal karyotype at diagnosis (Table 1); however, genomic copy number analysis, performed on CD138$^+$ cells, allowed the identification of CNV in 100% of the cases. A total of 270 copy number changes (ranging from 2 to 26) were found; 145 were copy number gains and 125 were losses. The median size of the aberration was 36 Mb (range, 0.026 Mb to 199 Mb). Gains most frequently involved chromosomes 19 (65%), 9 (42%), 15 (42%), 5 (38%), 3 (38%), 7 (35%) and 1q (38%), and losses in 13q (38%), 8p (35%), 16p (31%), 22q (31%) and 1p (27%). The most frequent aberrations were structural rearrangements involving chromosome segments (41.5% of the changes), followed by whole chromosome gains and losses (31.1%). There are two major genetic categories of MM: H-MM with 48 to 74 chromosomes due to specific chromosome gains and NH-MM without this genotype. Fifty percent of our cases were H-MM, the other fifty percent were NH-MM, initially assessed by array CGH and confirmed by conventional FISH (Table 1). Furthermore, unsupervised clustering, carried out with the most frequent aberrations found in our series, segregated two groups belonging to H-MM and NH-MM (*Supplementary Figure 1*). When H-MM and NH-MM cases were compared, we found that numerical changes were significantly more frequent in H-MM samples ($p<0.001$) due to a higher frequency of whole chromosome gains ($p<0.001$). However, monosomies seemed to be more frequent in the NH-MM group ($p=0.076$). As far as structural aberrations, we found that gains >3Mb were significantly more frequent ($p=0.037$) in H-MM cases (*Supplementary Table 3*). Other types of changes were equally distributed in both groups.

Clustering analysis identified two different H-MM subgroups

In order to obtain a reliable picture of common aberrations present in this series, we defined the SORI for gains and losses. Sixty-eight SORI were identified: 33 gains and 35 losses (Table 2). The most frequent gained SORI was 19p13.12-pter (65%) followed by 9q34, 19q13 and 19q13.2 (50%) and the most frequent losses were in 13q12-q21 (38%), 13q12.12 (35%), 8p12-p22 (27%) and 16p13.12 (23%). The median size was 1.5 Mb ranging from 0.026 Mb (a few genes) to 102 Mb (whole chromosomes). Deletion at 16p13.12, present in 23% of the cases, affected only *ERCC4*, a modifier gene reported to be

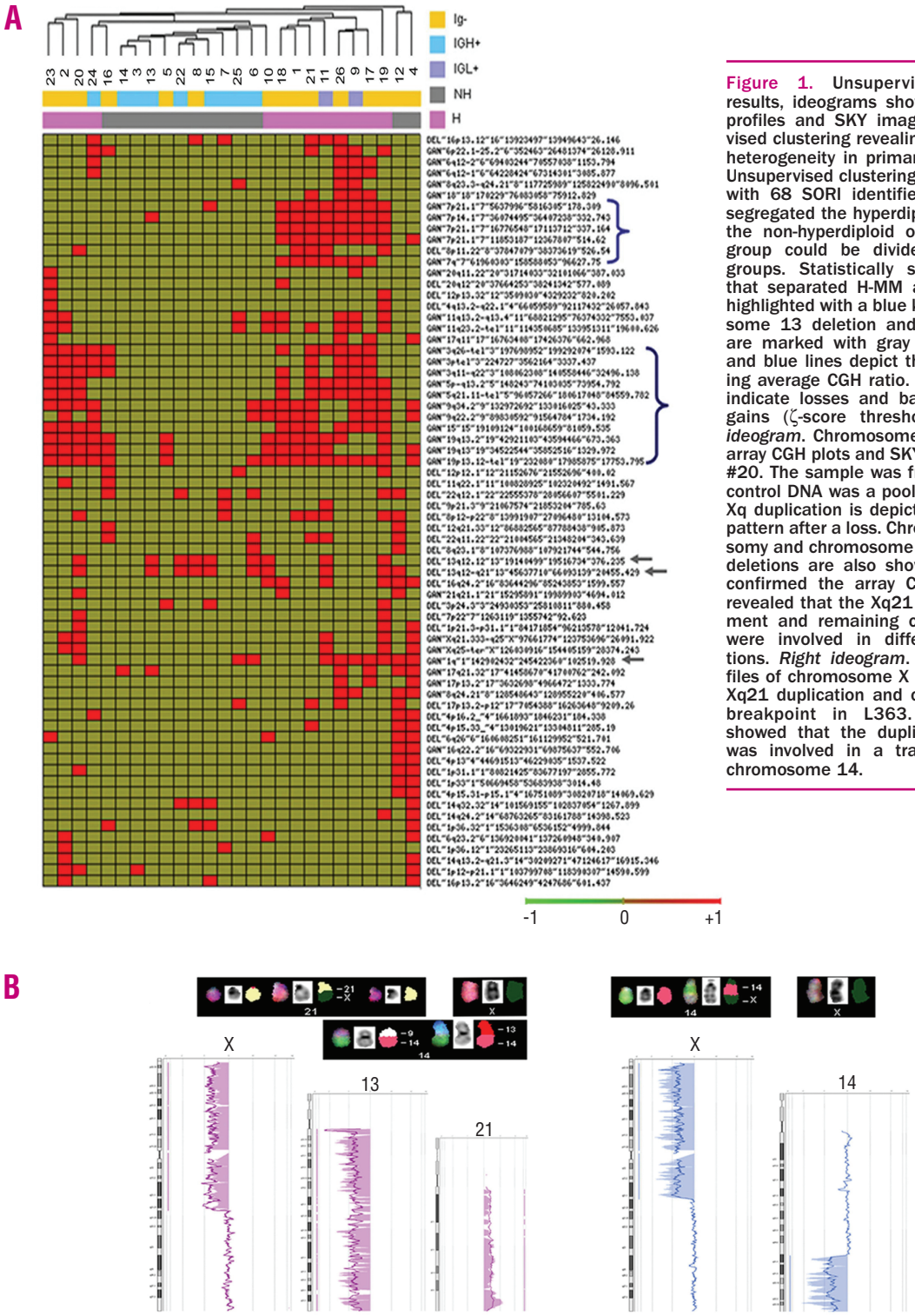

Figure 1. Unsupervised clustering results, ideograms showing array CGH profiles and SKY images. **A.** Unsupervised clustering revealing the molecular heterogeneity in primary MM samples. Unsupervised clustering was carried out with 68 SORI identified. The analysis segregated the hyperdiploid cases from the non-hyperdiploid ones. The H-MM group could be divided in two subgroups. Statistically significant SORI that separated H-MM and NH-MM are highlighted with a blue key, and chromosome 13 deletion and 1q duplication are marked with gray arrows. **B.** Red and blue lines depict the 500 Kb moving average CGH ratio. Bars on the left indicate losses and bars on the right gains (ζ-score threshold of 2). *Left ideogram*. Chromosomes X, 13 and 21 array CGH plots and SKY picture of case #20. The sample was from a male, the control DNA was a pool of female DNA. Xq duplication is depicted as a normal pattern after a loss. Chromosome 21 trisomy and chromosome 13 homozygous deletions are also shown. SKY assays confirmed the array CGH results and revealed that the Xq21 duplicated fragment and remaining chromosome 13 were involved in different translocations. *Right ideogram*. Array CGH profiles of chromosome X and 14 showing Xq21 duplication and chromosome 14 breakpoint in L363. SKY analysis showed that the duplicated fragment was involved in a translocation with chromosome 14.

involved in breast cancer.[15] Unsupervised and supervised clustering analyses were performed using SORI as variables (Figure 1A). Unsupervised analysis was able to segregate H-MM from NH-MM, and after a supervised analysis, gained regions in chromosomes 15, 5, 19, 3, 9, 7 and 11q were found to be significantly (adjusted p-value <0.05) more frequent in the H-MM group. In the unsupervised analysis, our H-MM cases appeared to be distributed in two subgroups that statistically differed (adjusted p-value=0.03, Fisher's exact test) according to the presence of gains in chromosome 7. Similarly, the unsupervised clustering analysis segregated two different subgroups within the NH-MM cases. One of the clusters, formed of only two cases, was characterized by the presence of a high number of CNV, such as gains in 8q24.21 (C-MYC) and absence of *IGH* translocations.

New genomic aberrations in MM

High level amplifications and homozygous deletions represented 7% of the observed CNV. They appeared in H-MM and NH-MM, but, in general, clustered in cases that accumulated a high number of genomic aberrations. Nine high level amplifcations were found and most of these regions were also gained (Table 3) in other cases from our series. Among the genes contained in all the amplified regions, 31% are involved in signal transduction (*GO:0007165*), such as *DIRAS2, ADORA2B, TNFRSF13B, RALGDS, CCNE1* and *SYK*. Six homozygous deletions were observed (Table 3). Reinforcing the putative pathogenic role of this finding, these regions also showed up as single copy losses in several additional samples of our series. Of interest, we observed a 376 Kb homozygous deletions in chromosome 13, where four genes (*HSMPP8, PSPC1, ZNF237, ZNF198*) are located (Table 2). This deletion was observed in two cases (#15 and 20). Case #20 showed a single copy of chromosome 13 that was involved in a translocation with chromosome 14 (Figure 1). Case #15 showed a homozygous deletions that included two consecutive clones involving only *ZNF198*. In general, the genes are involved in cellular physiological processes (*GO:0050875*), although some of them are more specifically involved in cell death (*GO:0008219*) and signal transduction (*GO:0007165*), such as *BIRC2, BIRC3* and *MAP3K5*; and others are metalloendopeptidases (*GO:0008237*) such as *MMP8, MMP10, MMP1* and *MMP13*. These high level amplifications and homozygous deletions were validated by FISH assays using BAC clones covering genes in lost or gained regions (*Supplementary Figure 2*).

A novel duplication on Xq21.33 was identified in five out of the 26 primary cases and in the MM cell line L363. FISH studies allowed the mapping of the duplication breakpoints that clustered around a 10 Mb region in Xq21.33 (from nearly 86122579bp to 98277428 bp). SKY analysis (Figure 1) demonstrated that duplications were the unbalanced outcome of translocations with breakpoints at Xq21: in L363 involving chromosome 14q, t(X;14)(q21.33; q31.1); and in case #20 involving chromosome 21; t(X;21)(q21.33;q22.3). The breakpoint in chromosome 14 was revealed out by the array CGH profile and we confirmed that *IGH* was not involved by using a combination of a chromosome X painting probe (Qbiogene) and the LSI IGH Dual Color Break Apart probe (Vysis) in the same hybridization (*Supplementary Figure 2*).

Discussion

Multiple myeloma is an incurable malignant plasma cell neoplasia characterized by the accumulation of malignant plasma cells in the bone marrow. Genetically, MM is defined by a large and variable number of genetic and chromosome rearrangements. In general, two major genetic subtypes of MM have been defined: the hyperdiploid variant associated with multiple chromosome trisomies and the non-hyperdiploid variant with a high prevalence of *IGH* translocations.[5] While the biology of MM bearing *IGH* translocations has been extensively studied,[16] little is known about the impact of genomic gains and losses in the pathogenesis of MM . In this regard, candidate genes, overexpressed in amplified chromosomal regions in MM cells lines have recently been proposed.[9] These events have been described in other types of cancer and have been used as therapeutic targets.

In this study, an array CGH platform was used for the analysis of copy number imbalances in CD138^{+} plasma cells. Although, as expected, most of the samples showed an unaltered karyotype at diagnosis, we found CNV in all of them. Observed frequencies of CNV, losses of chromosome 13q and duplications of chromosome 1q, and Ig genes translocations, were concordant with those in previous studies.[6,7,9,12,17] Array CGH enabled efficient segregation of the series into H-MM and NH-MM cases; half of the cases were H-MM and half NH-MM. The presence of *IGH* translocations was associated with NH-MM; among the H-MM cases, only one showed *IGH* translocations and two *IGL* translocations. It has been suggested that translocations present in H-MM are secondary events.[5,17]

Array CGH provides a level of resolution that overcomes the limits of chromosome-based CGH which is, in the best conditions, near 3 Mb. Due to the high resolution of the platform (44K) we identified several aberrations smaller than this limit, distributed in both H-MM and NH-MM cases, which had not been previously described. We delimited several SORI, offering a reliable picture of the aberrations occurring in MM.[12] Apart from segregating the two major genetic categories of MM, the unsupervised clustering based on the SORI aberration (Figure 1A) identified two H-MM subgroups, one of which was associated with chromosome 7 gains. Gains in 7q have been described in Burkitt´s lymphoma,[18] a combination in which they were associated with a poor outcome.

The approach used also allowed the identification of novel genomic markers and the definition of high level amplifications and homozygous deletions. Nine high level amplifications were identified. Some of them, such as 9q22.2, 19q13 and 16q22.2, had not been previously described in MM, but may harbor candidate oncogenes, as we have demonstrated in mantle cell lymphoma, in which we observed primary samples showing amplification and overexpression of *SYK*,[19] or *CCNE1*, in 19q13, which has been shown to be amplified and overexpressed in endometrial and bladder neoplasia.[20,21] Most of the homozygous deletions we found had not been previously described in MM. Reinforcing the putative pathogenic role of this finding, these regions also showed up as single copy losses in several additional samples of our series. As regards homozygous deletion in chromosome 13, *ZNF198* seems to be a good candidate for the target of the deletion because, besides the deletion described in case #20, in case #15, the homozygous dele-

tion covered only the *ZNF198* gene. Furthermore, candidate genes such as *PORIMIN*, *YAP1* and *MMP8*, which are located in the homozygous deletion that we found at 11q22.2, were reported to be deleted and down regulated in a previous study. Five cases showed duplication on Xq21.33. Although some CGH studies have reported data on Xq aberrations,[22,23] we provide here the first description of the frequency and genetic origin of this marker in MM. In summary, our study represents the analysis of CNV in MM at the highest level of resolution ever reported. Our work includes some data confirming results obtained with other technological approaches, and provides a complete genomic characterization of the two genetic categories of MM. Additionally, we have demonstrated for the first time that extreme genomic aberrations, such as high level amplifications and homozygous deletions, are frequent events in MM. We believe that these data warrant further investigation to gain a deeper insight into the role of genomic instability in MM and its potential use for therapeutic purposes.

Authors' Contributions

CL carried out all technical arrays, SKY and some FISH experiments. She contributed to the writing of the paper; BS performed FISH assays and contributed to the writing the paper; SA designed the study and contributed to the microarray analisis of the data; JS, BF and DB carried out microarray analyses and contributed to the analysis of the data; FP has sustantially contributed substantially with biological material and clinical data; MJC contributed with essential biological material, cytogenetic information and helped to design the experiments; JCC designed the work, collected all data and wrote the paper.

Conflict of Interest

The authors reported no potential conflicts of interest.

References

1. Kyle RA, Rajkumar SV. Multiple myeloma. N Engl J Med 2004; 351: 1860-73.
2. Seidl S, Kaufmann H, Drach J. New insights into the pathophysiology of multiple myeloma. Lancet Oncol 2003;4:557-64.
3. Kuehl WM, Bergsagel PL. Multiple myeloma: evolving genetic events and host interactions. Nat Rev Cancer 2002;2:175-87.
4. Fonseca R, Barlogie B, Bataille R, Bastard C, Bergsagel PL, Chesi M, et al. Genetics and cytogenetics of multiple myeloma: a workshop report. Cancer Res 2004;64:1546-58.
5. Chng WJ, Santana-Davila R, Van Wier SA, Ahmann GJ, Jalal SM, Bergsagel PL, et al. Prognostic factors for hyperdiploid-myeloma: effects of chromosome 13 deletions and IgH translocations. Leukemia 2006; 20: 807-13.
6. Cigudosa JC, Rao PH, Calasanz MJ, Odero MD, Michaeli J, Jhanwar SC, et al. Characterization of nonrandom chromosomal gains and losses in multiple myeloma by comparative genomic hybridization. Blood 1998; 91:3007-10.
7. Gutierrez NC, Garcia JL, Hernandez JM, Lumbreras E, Castellanos M, Rasillo A, et al. Prognostic and biologic significance of chromosomal imbalances assessed by comparative genomic hybridization in multiple myeloma. Blood 2004;104:2661-6.
8. Rao PH. Comparative genomic hybridization for analysis of changes in DNA copy number in multiple myeloma. Methods Mol Med 2005; 113:71-83.
9. Largo C, Alvarez S, Saez B, Blesa D, Martin-Subero JI, Gonzalez-Garcia I, et al. Identification of overexpressed genes in frequently gained/amplified chromosome regions in multiple myeloma. Haematologica 2006; 91: 184-91.
10. Martin-Subero JI, Harder L, Gesk S, Schlegelberger B, Grote W, Martinez-Climent JA, et al. Interphase FISH assays for the detection of translocations with breakpoints in immunoglobulin light chain loci. Int J Cancer 2002;98:470-4.
11. Barrett MT, Scheffer A, Ben-Dor A, Sampas N, Lipson D, Kincaid R, et al. Comparative genomic hybridization using oligonucleotide microarrays and total genomic DNA. Proc Natl Acad Sci USA 2004;101:17765-70.
12. Carrasco DR, Tonon G, Huang Y, Zhang Y, Sinha R, Feng B, et al. High-resolution genomic profiles define distinct clinico-pathogenetic subgroups of multiple myeloma patients. Cancer Cell 2006;9:313-25.
13. Rodriguez-Perales S, Martinez-Ramirez A, de Andres SA, Valle L, Urioste M, Benitez J, et al. Molecular cytogenetic characterization of rhabdomyosarcoma cell lines. Cancer Genet Cytogenet 2004;148:35-43.
14. Rao PH, Cigudosa JC, Ning Y, Calasanz MJ, Iida S, Tagawa S, et al. Multicolor spectral karyotyping identifies new recurring breakpoints and translocations in multiple myeloma. Blood 1998;92:1743-8.
15. Smith TR, Levine EA, Perrier ND, Miller MS, Freimanis RI, Lohman K, et al. DNA-repair genetic polymorphisms and breast cancer risk. Cancer Epidemiol Biomarkers Prev 2003;12: 1200-4.
16. Bergsagel PL, Kuehl WM. Molecular pathogenesis and a consequent classification of multiple myeloma. J Clin Oncol 2005;23:6333-8.
17. Smadja NV, Fruchart C, Isnard F, Louvet C, Dutel JL, Cheron N, et al. Chromosomal analysis in multiple myeloma: cytogenetic evidence of two different diseases. Leukemia 1998;12:960-9.
18. Garcia JL, Hernandez JM, Gutierrez NC, Flores T, Gonzalez D, Calasanz MJ, et al. Abnormalities on 1q and 7q are associated with poor outcome in sporadic Burkitt's lymphoma. A cytogenetic and comparative genomic hybridization study. Leukemia 2003;17:2016-24.
19. Rinaldi A, Kwee I, Taborelli M, Largo C, Uccella S, Martin V, et al. Genomic and expression profiling identifies the B-cell associated tyrosine kinase Syk as a possible therapeutic target in mantle cell lymphoma. Br J Haematol 2006;132:303-16.
20. Cassia R, Moreno-Bueno G, Rodriguez-Perales S, Hardisson D, Cigudosa JC, Palacios J. Cyclin E gene (CCNE) amplification and hCDC4 mutations in endometrial carcinoma. J Pathol 2003;201:589-95.
21. Richter J, Wagner U, Kononen J, Fijan A, Bruderer J, Schmid U, et al. High-throughput tissue microarray analysis of cyclin E gene amplification and overexpression in urinary bladder cancer. Am J Pathol 2000;157:787-94.
22. Inoue J, Otsuki T, Hirasawa A, Imoto I, Matsuo Y, Shimizu S, et al. Overexpression of PDZK1 within the 1q12-q22 amplicon is likely to be associated with drug-resistance phenotype in multiple myeloma. Am J Pathol 2004;165:71-81.
23. Liebisch P, Viardot A, Bassermann N, Wendl C, Roth K, Goldschmidt H, et al. Value of comparative genomic hybridization and fluorescence in situ hybridization for molecular diagnostics in multiple myeloma. Br J Haematol 2003;122:193-201.